International Journal of Pharmaceutics 650 (2024) 123706

Contents lists available at ScienceDirect

International Journal of Pharmaceutics

journal homepage: www.elsevier.com/locate/ijpharm

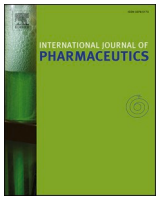

Vac-and-fill: A micromoulding technique for fabricating microneedle arrays with vacuum-activated, hands-free mould-filling

Emma Smith [a,b], Wing Man Lau [a,b], Tarek M. Abdelghany [c,d,e], Djurdja Vukajlovic [f], Katarina Novakovic [f], Keng Wooi Ng [a,b,*]

[a] School of Pharmacy, Newcastle University, King George VI Building, Newcastle upon Tyne NE1 7RU, United Kingdom
[b] Translational and Clinical Research Institute, Newcastle University, Newcastle upon Tyne NE1 7RU, United Kingdom
[c] Department of Pharmacology and Toxicology, Faculty of Pharmacy, Cairo University, Kasr El-Aini St., Cairo 11562, Egypt
[d] Institute of Education in Healthcare and Medical Sciences, School of Medicine, Medical Sciences and Nutrition, University of Aberdeen, Foresthill, Aberdeen AB25 2ZD, United Kingdom
[e] School of Biomedical, Nutritional and Sport Sciences, Faculty of Medical Sciences, Newcastle University, Newcastle Upon Tyne NE24HH, United Kingdom
[f] School of Engineering, Newcastle University, Newcastle upon Tyne NE1 7RU, United Kingdom

ARTICLE INFO

Keywords:
Polymer microneedle
Micromolding
Vacuum
Liquid formulation
Pressure

ABSTRACT

We report a simple and reproducible micromoulding technique that dynamically fills microneedle moulds with a liquid formulation, using a plastic syringe, triggered by the application of vacuum ('vac-and-fill'). As pressure around the syringe drops, air inside the syringe pushes the plunger to uncover an opening in the syringe and fill the microneedle mould without manual intervention, therefore removing inter-operator variability. The technique was validated by monitoring the plunger movement and pressure at which the mould would be filled over 10 vacuum cycles for various liquid formulation of varying viscosity (water, glycerol, 20 % polyvinylpyrrolidone (PVP) solution or 40 % PVP solution). Additionally, the impact of re-using the disposable syringes on plunger movement, and thus the fill pressure, was investigated using a 20 % PVP solution. The fill pressure was consistent at 300–450 mbar. It produced well-formed and mechanically robust PVP, poly(methylvinylether/maleic anhydride) and hydroxyethylcellulose microneedles from liquid formulations. This simple and inexpensive technique of micromoulding eliminated the air entrapment and bubble formation, which prevent reproducible microneedle formation, in the resultant microneedle arrays. It provides a cost-effective alternative to the conventional micromoulding techniques, where the application of vacuum ('fill-and-vac') or centrifugation following mould-filling may be unsuitable, ineffective or have poor reproducibility.

1. Introduction

Microneedles are micron-sized needles attached to a backing/patch that are used in drug delivery. The microneedles are long enough that, when inserted into the skin, they perforate the stratum corneum and deliver drugs to the dermal microcirculation (Larrañeta et al., 2016), yet short enough to not cause bleeding or pain (Gill et al., 2008; Haq et al., 2009; Kaushik et al., 2001). Microneedles were first introduced in the 1970 s (Gerstel and Place, 1976). Their development accelerated in the 1990 s due to the growth in the microelectronics industry and the availability of microfabrication techniques (Arora et al., 2008). Different types of microneedles have been developed, including solid, hollow, coated, dissolving and hydrogel-forming microneedles made from various polymers, such as polyvinylpyrrolidone (PVP) (Sullivan et al., 2010), hyaluronic acid (HA) (Liu et al., 2012), carboxymethyl cellulose (CMC) (Lee et al., 2008), chitosan (Xie et al., 2005) and poly (methyl vinyl ether-co-maleic) acid (Donnelly et al., 2014, 2012).

The most widely used method for manufacturing dissolving microneedles and hydrogel-forming microneedles is micromoulding by solvent casting, due to its simple process at ambient temperatures (Singh et al., 2019). Microneedle moulds are commonly made from polydimethylsiloxane (PDMS), which is cast onto a master template microneedle array to form a negative mould (McAllister et al., 2003). The polymer formulation, in the form of a liquid solution, is then cast into the PDMS mould (Wang et al., 2022). A subsequent degassing step is usually necessary to remove air from the microcavities within the

* Corresponding author.
E-mail address: keng.ng@newcastle.ac.uk (K.W. Ng).

https://doi.org/10.1016/j.ijpharm.2023.123706
Received 25 August 2023; Received in revised form 21 November 2023; Accepted 12 December 2023
Available online 14 December 2023

mould, by the application of vacuum (Lau et al., 2017; Tas et al., 2017) or centrifugation (Abdelghany et al., 2019; Zhao et al., 2018) to enable the liquid formulation to enter the microcavities, displacing any air, to form the microneedles. The liquid formulation is then dried by solvent evaporation to form a microneedle array (Tucak et al., 2020). In this process, the effective removal of air from the mould, as well as the liquid formulation itself, is necessary to ensure the formation of the microneedles and content uniformity in the microneedle formulation.

Micromoulding using the solvent casting method followed by vacuum ('fill-and-vac') has produced varying results depending on the physical properties of the liquid formulation (e.g., viscosity). Specifically, we have encountered air bubble entrapment in the formulation and incomplete air removal from the microcavities, despite extended incubation times at 100 mbar, resulting in a failure to form microneedles and air pockets in the backing material (base plate) of the dried microneedle array. Similarly, Martin et al. (2012) reported that incubating the filled moulds at 300 mbar for 60 min did not sufficiently remove the air from the microcavities in the mould, which led to incomplete microneedle formation. The number of completely formed microneedles varied greatly between attempts, and a fully formed microneedle array was never produced across at least 6 experiments. Martin et al. (2012) ascribed the problem to the high surface tension of the liquid formulation, which prevented it from flowing into the microcavities. In our case, the presence of air bubbles within the backing material itself suggests that the high viscosity of the formulation may also prevent efficient air removal from the body of the liquid. This is supported by Yang et al. (2012), who reported a similar observation while attempting, unsuccessfully, to remove air bubbles from a viscous solution containing 38 % polyvinyl alcohol:dextran (98:2) by applying vacuum.

To overcome this challenge, we have developed a new technique to fill the microneedle mould with the liquid formulation using a modified plastic syringe. Hands-free filling of the mould at a specific pressure is dynamically triggered by the application of vacuum. The evacuation of air from the mould *before* filling (the 'vac-and-fill' approach) avoids air entrapment in the formulation. Here, we report the method development, validation, and considerations for this new micromoulding technique.

2. Material and methods

2.1. Vacuum chamber

Unless otherwise stated, all vacuum procedures were performed at room temperature (~20 °C) in a 31 L vacuum oven (OVA031.XX3.5; Fistreem International, Cambridge, UK), rated 0–1000 mbar, with the heating turned off. Air was removed from the vacuum oven using a Fisherbrand® polytetrafluoroethylene diaphragm vacuum pump (Fisher Scientific, Loughborough, UK), with a nominal air displacement rate of 38 L per minute and maximum vacuum (minimum pressure) of 8 mbar.

2.2. Fabrication of PDMS moulds

Negative moulds of the microneedle array were fabricated from PDMS against an epoxy master as the positive mould, using a method adapted from McAllister et al. (2003) and optimised in our lab for our microneedle array designs (Ng et al., 2015; Skaria et al., 2019). Briefly, the Sylgard® 184 elastomer base was mixed with the curing agent (both from the Sylgard® 184 Silicone Elastomer Kit; The Dow Chemical Company, Wilmington, Delaware, USA) in a 10:1 mass ratio. The mixture was then degassed in the vacuum chamber for 15 min (100 mbar). Aluminium foil was moulded around the bottom of a 20 mL glass vial to create a basin. The microneedle master was then placed into the foil basin, with the microneedles facing up. The elastomer mixture was then poured over the epoxy master in the basin. The mixture in the foil basin was degassed again in the vacuum chamber for 30 min (100 mbar) and then placed on a hotplate at 100 °C for 30–60 min to cure. The foil basin was peeled away, and the epoxy master was carefully removed using tweezers to reveal the PDMS mould.

The epoxy masters used in this work were themselves replicated using a micromoulding technique, with PDMS moulds made in the same way as described above, against a steel master produced by computer numerical control (CNC) machining. The Agar 100 Resin Kit (Agar Scientific, Stansted, UK) was used to form hard epoxy masters using the manufacturer's standard formulation. Briefly, the Agar 100 epoxy resin, hardeners dodecenylsuccinic anhydride (DDSA) and methyl nadic anhydride (MNA) plus a 7 mL glass vial were prewarmed in a water bath (60 °C). Agar 100 epoxy resin, DDSA and MNA were then measured into the prewarmed vial using a 1 mL syringe. The content was then mixed by rotating the vial by hand for a few minutes. The benzyldimethylamine accelerator solution was then pipetted into the vial, mixed using a pipette tip, and then further mixed by rotating the vial by hand for a few minutes until the solution turned orange. The Agar 100 resin was then pipetted into PDMS moulds and degassed in a vacuum oven (Fistreem International, Cambridge, UK) until no air bubbles remained (30 °C, 100 mbar). The vacuum was then released, and the temperature was increased to 60 °C. The moulds were left to incubate for $\geq$ 18 h at 60 °C. Once the resin had set, the epoxy microneedle arrays were removed using tweezers. All epoxy masters were examined under a light microscope (CETI Steddy-T stereomicroscope; Medline Scientific, Oxon, UK) to confirm the microneedles were well-formed.

The epoxy microneedles had these nominal dimensions: shape = conical (with a flat tip); length = 925 μm; tip width = 140 μm; base width = 200 μm; pitch = 1.6 mm. They were arranged in a 5 × 5 grid on a circular disc-shaped backing material (base plate).

2.3. Liquid formulations

2.3.1. Preparation of polymer solutions

For initial method development, 20 % (w/v) and 40 % (w/v) PVP solutions were prepared by dissolving Plasdone™ k-29/32 (Ashland, Wilmington, Delaware, USA) in 20 % (v/v) ethanol (absolute; Fisher Scientific, Loughborough, UK) and 80 % (v/v) deionised water. Glycerol was used as supplied by Merck Life Science (Gillingham, UK).

A range of polymer solutions, with or without a drug payload, was then used to fabricate microneedle arrays using the 'vac-and-fill' technique to demonstrate its versatility. 15 % (w/v) poly(methylvinylether/maleic anhydride) (PMVE/MA) solution was prepared by dissolving Gantrez™ AN-139 (Ashland, Wilmington, Delaware, USA) in deionised water and stirring continuously at 95 °C until a clear gel formed (Donnelly et al., 2011). 0.7 % (w/v) hydroxyethylcellulose (HEC) solution was obtained by dissolving Natrosol™ (Ashland, Wilmington, Delaware, USA) in deionised water. Methylene blue (MB) and dexamethasone sodium phosphate (DSP) were used as the drug payload. Model drug solutions containing MB (20 mg/mL) or DSP (50 mg/mL) were prepared by dissolving the respective powders (Merck Life Science, Gillingham, UK) in deionised water. These drug solutions were then mixed with the polymer solutions at volume ratios between 1:49 and 1:10, to produce final drug concentrations ranging from 0.4 to 5 mg/mL (Table 1).

2.3.2. Viscosity assessment

For initial method development, the relative viscosity of deionised water, glycerol, 20 % PVP solution and 40 % PVP solution was assessed using the vial inversion method (Al Khateb et al., 2016). The liquid formulations were placed into separate 7 mL glass vials. The vials were inverted simultaneously, and the liquid formulations allowed to flow towards the lid. The flow rate of the liquid formulations was compared visually as a surrogate measure of relative viscosity. Furthermore, the shear viscosity of all liquid formulations was determined on the Kinexus Pro + rotational rheometer (Malvern Panalytical; Worcestershire, UK) at 20 °C, using a 4 cm cone and plate geometry, a gap size of 0.14 mm, and an increasing shear rate between 1 and 100 s^{-1}.

Table 1
The shear viscosity of different liquid polymer formulations, with or without MB or DSP as the drug payload, shown as mean ± standard deviation ($n = 21$). The polymer solution concentrations were reduced slightly following drug incorporation. The diluted polymer concentrations (w/v) are shown in parentheses.

Polymer solution	Drug content	Shear viscosity (Pa•s)
PVP, 20 %	–	0.0546 ± 0.0013
PVP, 20 % (18 %)	MB, 1 mg/mL	0.0376 ± 0.0032
PVP, 20 % (18 %)	DSP, 5 mg/mL	0.0499 ± 0.0006
PVP, 40 %	–	0.8996 ± 0.0034
PMVE/MA, 15 %	–	0.4483 ± 0.0381
PMVE/MA, 15 % (14.7 %)	MB, 0.4 mg/mL	0.3680 ± 0.0447
PMVE/MA, 15 % (14.7 %)	DSP, 1 mg/mL	0.3727 ± 0.1166
HEC, 0.7 %	–	0.0950 ± 0.0206
HEC, 0.7 % (0.69 %)	DSP, 1 mg/mL	0.3052 ± 0.0978
Glycerol	–	0.3491 ± 0.0109

2.4. Conventional 'fill-and-vac' micromoulding

Using a 1 mL syringe, 0.3–0.4 mL of the 20 % PVP solution was placed into a PDMS microneedle mould. The PDMS mould was then placed into the vacuum chamber for 15 min at 100 mbar. The vacuum was then turned off. This was repeated two more times for a total of 45 min in the vacuum.

2.5. New 'vac-and-fill' micromoulding

2.5.1. Apparatus

The apparatus shown in Fig. 1 was placed in the vacuum chamber. To prepare the apparatus, the tip of a Fisherbrand® 5 mL polypropylene syringe was cut off with scissors, and another plunger (the lower plunger) from an identical syringe was inserted through the cut opening. To enable mould-filling, a circular hole (diameter = 4 mm) was drilled into the syringe barrel, opposite the 1 mL mark, using an electric hand drill. During use, the lower plunger was inserted deep into the syringe barrel to conceal the drilled hole. The upper plunger was static and was only used to adjust the air and liquid volume when filling the syringe. The syringe, with both plungers fitted, was placed onto a 3D-printed syringe holder (see Supplementary Information) with the original plunger (the upper plunger) fully extended and pointing upwards at a 20.3° angle. The PDMS microneedle mould was positioned directly below the drilled hole.

As vacuum was applied and the pressure outside the syringe gradually dropped, the greater pressure inside the syringe pushed the lower plunger out gradually until the pressure was equalised, causing the air inside the syringe to expand at the same time. For calibration, the initial amount of air in the syringe was adjusted so that the lower plunger would move at an appropriate rate to uncover the drilled hole at the desired pressure. The liquid formulation then flowed out through the hole into the mould below. At the same time, the air from within the syringe escaped through the same hole and pushed the liquid formulation out from behind until the pressure was equalised. Thus, the flow of the liquid formulation into the mould was driven by a combination of: (1) suction, i.e., escaping air pushing the liquid formulation out due to the pressure differential between the inside and outside of the syringe; and (2) gravity.

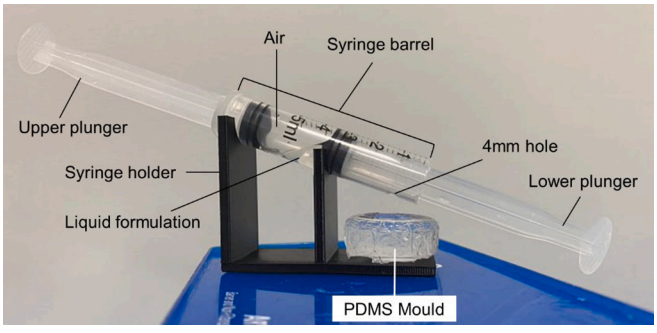

Fig. 1. The apparatus designed to trigger hands-free filling of the mould at a specific pressure, in response to the application of vacuum.

2.5.2. Effect of liquid formulation on plunger movement

The initial volume of air in the syringe was carefully calibrated to ensure the right amount of air expansion, so that the lower plunger would travel the appropriate distance to uncover the drilled hole consistently at an appropriate pressure. We hypothesised that the viscosity of the liquid formulation in the syringe may affect plunger movement. Thus, the initial experiments sought to determine the consistency of plunger movements in syringes containing liquid formulations of differing viscosity. These experiments were performed with new syringes (including both new plungers) without the drilled hole in the barrel, since no actual mould-filling was necessary.

For the syringes containing air only (as calibration), the upper plunger was fully extended out while the lower plunger was positioned at the 4 mL mark (see Supplementary Information for full calibration details). For the syringes containing 2 mL of air plus a liquid formulation (deionised water, glycerol, 20 % PVP solution or 40 % PVP solution), the upper plunger was firstly positioned at the 4 mL mark. Then, using a 1 mL syringe, 0.5 mL of the liquid formulation was dispensed into the syringe barrel. The lower plunger was then pushed in until the upper plunger was fully extended at the opposite end, and the lower plunger rested at the 3.4–3.6 mL mark. This corresponded to ~ 2 mL air in the syringe barrel. The apparatus was placed into the vacuum chamber. Air was removed from the vacuum chamber until the lower plunger cleared the 0.9 mL mark (i.e., the plunger position necessary to fully uncover the drilled hole). The pressure at which this happened was read off the pressure gauge of the vacuum chamber. The vacuum pump was then turned off. The upper and lower plungers were reset to their starting positions as described above, without replacing the contents of the syringe, and the process was repeated for 10 vacuum cycles.

2.5.3. Effect of re-using syringes

To investigate whether the syringes could be re-used to produce consistent results, the plunger movement of used syringes (fitted with used plungers) in response to the pressure drop was determined. The used syringes and plungers from Section 2.5.2 were rinsed thoroughly in tap water, air-dried, and filled with 1.1 mL air plus 0.5 mL 20 % PVP solution. The apparatus in Section 2.5.1 was assembled with these used syringes, placed in the vacuum chamber, and subjected to 10 vacuum cycles at 100 mbar. The plunger movement was recorded as the volume displacement (in mL, read off the graduation on the syringe barrel) when the lower plunger stopped moving at 100 mbar.

2.6. Formation and characterisation of microneedle arrays

2.6.1. Microneedle array fabrication

PDMS moulds were filled using the conventional 'fill-and-vac' method (Section 2.4) or the new 'vac-and-fill' method. For the latter, the procedure in Section 2.5.2 was repeated to fill the liquid formulations (Section 2.3.1) into PDMS moulds, using new syringes (including both new plungers) with the 4 mm drilled hole in the barrel. The moulds filled using both methods were examined visually for air bubbles in the liquid formulation. The formulations were then air-dried at ~ 20 °C to form microneedle arrays. The dried microneedles arrays were carefully removed from the mould using tweezers.

2.6.2. Light microscopy

The microneedle arrays were examined under a light microscope (CETI Steddy-T stereomicroscope; Medline Scientific, Oxon, UK). Images were captured using an 18-megapixel D18 digital camera controlled with the ToupLite software (Medline Scientific, Oxon, UK).

2.6.3. Texture analysis

The axial failure force (AFF) of individual PVP microneedles (without MB or DSP) was measured on the TA.XTplusC texture analyser fitted with a video capture and synchronisation system (Stable Micro systems, Surrey, UK). The texture analyser was set to compression mode, with a 2 mm-diameter probe, a test speed of 0.1 mm•s^{-1}, a trigger force of 0.001 N and a maximum force of 50 N. The microneedle array was clamped in a holder with the microneedles upright, tips facing upwards. The microneedle of interest was positioned directly below the probe. During compression, the probe lowered towards the single microneedle, compressing it between the probe and the base plate of the microneedle array. The AFF of the microneedle was determined from the first peak in the force–displacement graph (Park et al., 2005). The failure (e.g., fracture, deformation) of the microneedle was corroborated visually from the synchronous video recording (Fig. 2). This procedure was performed on forty microneedles individually across 4 PVP microneedle arrays (i.e., 10 microneedles per array).

2.6.4. Skin penetration test

Pig ears were obtained as a waste product of the farming industry. Full-thickness skin was harvested from the back of the ears as described previously (Lau et al., 2012) and frozen at −80 °C. The skin was fully defrosted at room temperature for 30 min before use. The skin was stretched and the PVP microneedle array was pressed into the skin using thumb pressure for 30 s. The microneedle array was left in situ and imaged using optical coherence tomography (OCT; Lumedica LabScope 2.0, Edmund Optics, York, UK).

2.7. Statistical analysis

Numerical experimental data were tabulated, and descriptive statistics generated in Microsoft Excel (Microsoft Corporation, Redmond, WA, USA). Statistical tests were performed in GraphPad Prism version 6.05 (GraphPad Software, La Jolla, CA, USA), at $\alpha = 0.05$.

3. Results

3.1. Conventional 'fill-and-vac' micromoulding

Fig. 3 shows a PDMS microneedle mould containing 20 % PVP solution at various stages of the vacuum cycle. The microcavities were clearly visible but there was no air bubble in the liquid formulation before vacuum was applied (Fig. 3A). After 15 min in the vacuum, air bubbles appeared in the liquid formulation at positions corresponding to the microcavities in the mould, suggesting that air entrapped within the microcavities had risen into the body of the liquid formulation. These bubbles remained after cycling through vacuum (100 mbar) for 30 min and 45 min, their positions having shifted somewhat after each vacuum cycle, but they had not escaped the liquid formulation (Fig. 3B–D). When dried, such formulations produced defective microneedle arrays (Section 3.3).

3.2. New 'vac-and-fill' micromoulding

3.2.1. Viscosity assessment

With the vial inversion method, the more viscous the liquid, the more slowly it would flow from the bottom of the vial towards the lid when inverted. Fig. 4 shows the inverted vials containing 3 mL of the liquid formulations (deionised water, 20 % PVP solution, 40 % PVP solution and glycerol). From the relative amounts of the liquids present at the bottom, side and top (near the lids) of the inverted vials and their relative flow rates, the relative viscosity of the liquids can be ranked in the following increasing order: deionised water < 20 % PVP < 40 % PVP ≈ glycerol. This was generally consistent with the rheological data for these liquid formulations, except the latter showed that the 40 % PVP solution was markedly more viscous than glycerol (Table 1). All other liquid formulations tested were less viscous than the 40 % PVP solution but most were more viscous than the 20 % PVP solution. Details of the shear viscosity measurements are provided in the Supplementary Information.

3.2.2. Effect of liquid formulation on plunger movement

Fig. 5 shows the fill pressure (i.e., the pressure at which the lower

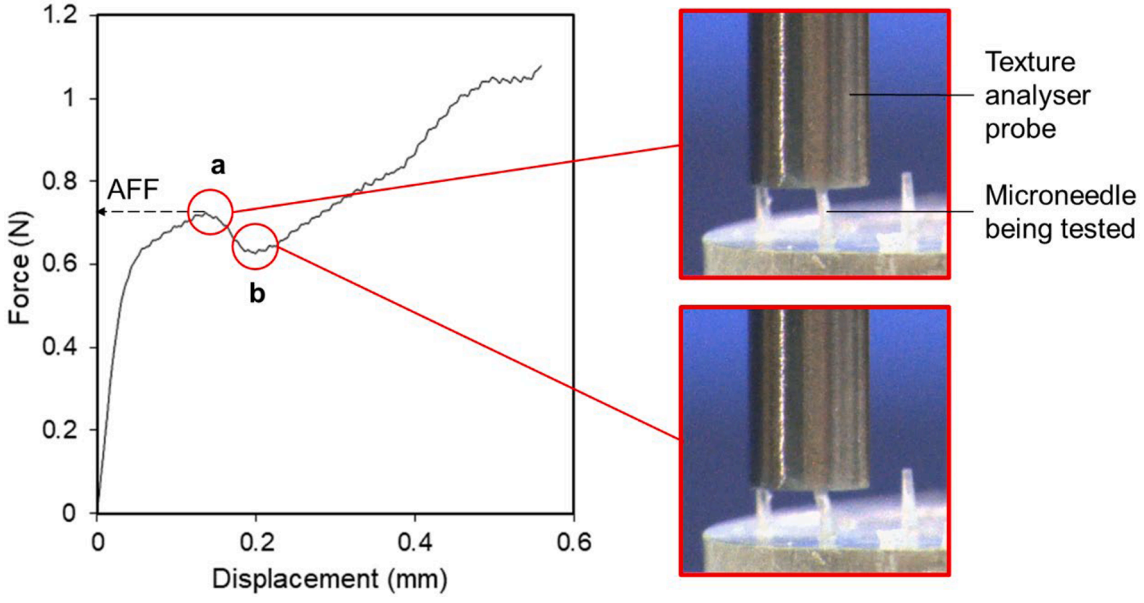

Fig. 2. Exemplar force–displacement graph (left) illustrating the determination of the AFF of a microneedle from the first peak (position a), corroborated by a synchronous video recording of the test (still frames from the video on the right). The microneedle being tested was positioned directly below the texture analyser probe. The adjacent microneedles were outside the perimeter of the probe and were never in contact with the probe during the test. At position b, the AFF had been exceeded and the tip of the microneedle being tested was visibly bent.

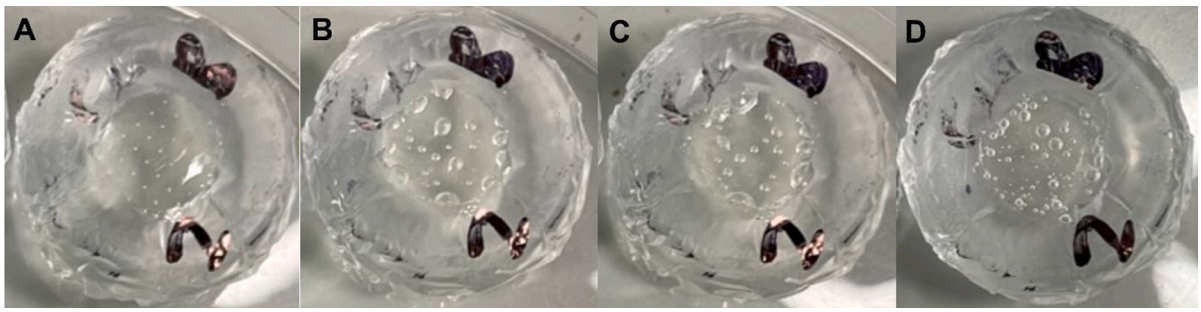

Fig. 3. A microneedle mould containing 0.5 mL 20 % PVP solution, filled using the conventional 'fill-and-vac' micromoulding technique, at various stages of the vacuum cycling process: (A) before application of vacuum, (B) after 15 min of vacuum, (C) after 30 min of vacuum, (D) after 45 min of vacuum (100 mbar, ~20 °C).

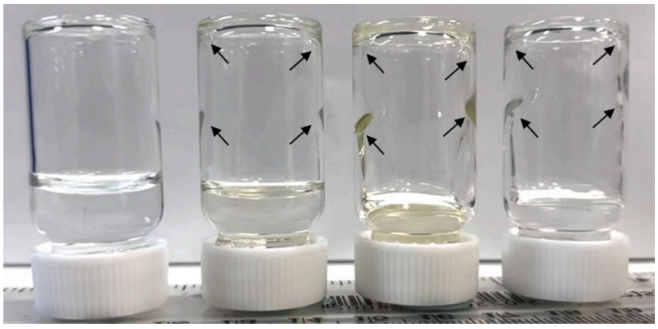

Fig. 4. Initial assessment of relative viscosity using the vial inversion method during method development: (left to right) deionised water, 20 % PVP solution, 40 % PVP solution and glycerol. The liquid volume in each vial was 3 mL and the vials were inverted simultaneously. The arrows denote residual liquid which was still flowing towards the lid when the image was captured.

plunger cleared the 0.9 mL mark to fully uncover the 4 mm hole) with the new 'vac-and-fill' technique using the apparatus in Fig. 1. This pressure was consistent over 10 vacuum cycles for air, deionised water, 20 % PVP solution, 40 % PVP solution and glycerol (Fig. 5A). For convenience, plunger movement was measured in terms of the volume displacement (in mL) read off the graduation on the syringe barrel. With the syringes containing air only, the lower plunger moved the furthest as it contained no liquid formulation and the lower plunger started at the 4 mL mark, moving a total of 2.9 mL. With the syringes containing the liquid formulations, the lower plunger started at 3.4 mL and moved 2.5 mL consistently. The average pressure (average of 10 vacuum cycles for each formulation, in mbar) at which the lower plunger moved enough to fully uncover the drilled hole is shown in Fig. 5B.

A two-way analysis of variance (ANOVA) with repeated measures and Tukey's test for multiple comparisons suggests that the fill pressure was not significantly different ($p = 0.17$) between the vacuum cycles within any formulation. However, there were statistically significant differences in the fill pressure between the liquid formulations ($p < 0.05$) within the vacuum cycles. Specifically, within the first 3 vacuum cycles, the plunger cleared the 0.9 mL mark at a significantly higher pressure with 40 % PVP solution than with glycerol. A statistically significant difference was also found between deionised water and glycerol at various stages of the vacuum cycle, with $p < 0.001$ in the first two cycles. Generally, more statistically significant differences were found between the formulations in the earlier cycles. As the vacuum cycles advanced, the fill pressure between the formulations converged and the differences gradually disappeared.

3.2.3. *Effect of re-using syringes*

Fig. 6 shows the lower plunger movement (as volume displacement in mL) over 10 vacuum cycles with re-used syringes containing 20 % PVP solution. The lower plunger movement was variable between the re-used syringes but the overall decrease over 10 vacuum cycles was observed in all syringes (Fig. 6A). This was in stark contrast to new syringes, which showed remarkable consistency in the plunger movement in response to the pressure drop over 10 vacuum cycles (Section 3.2.2). The volume displacement at 100 mbar (rather than the pressure at

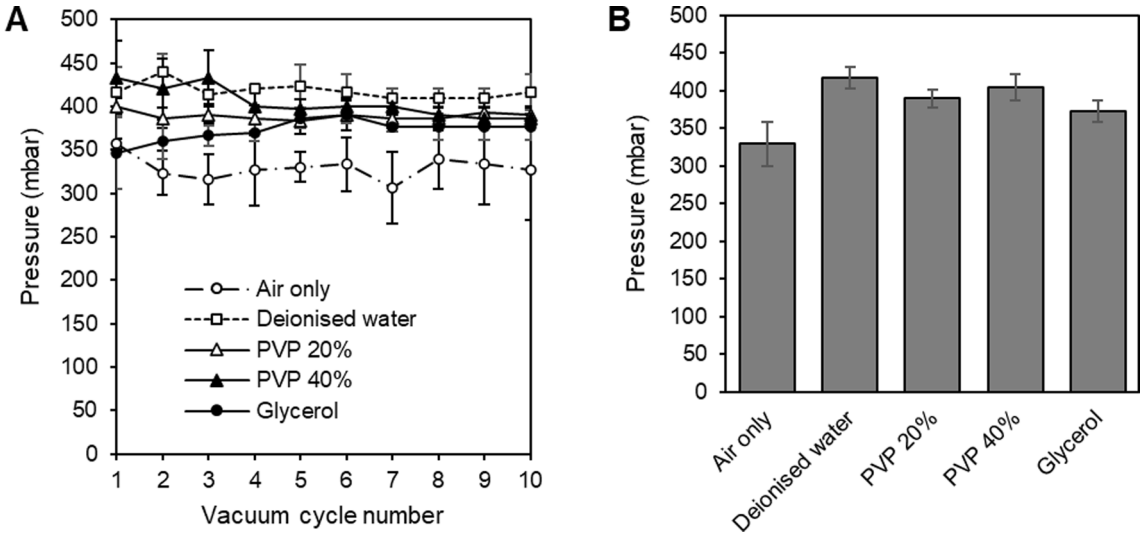

Fig. 5. Pressure at which the lower plunger cleared the 0.9 mL mark, sufficient to fully uncover the 4 mm drilled hole to allow the various liquid formulations to fill the mould: (A) over 10 vacuum cycles. (B) the average of 10 vacuum cycles per syringe. Data are mean ± standard deviation ($n = 3$ new syringes and plungers).

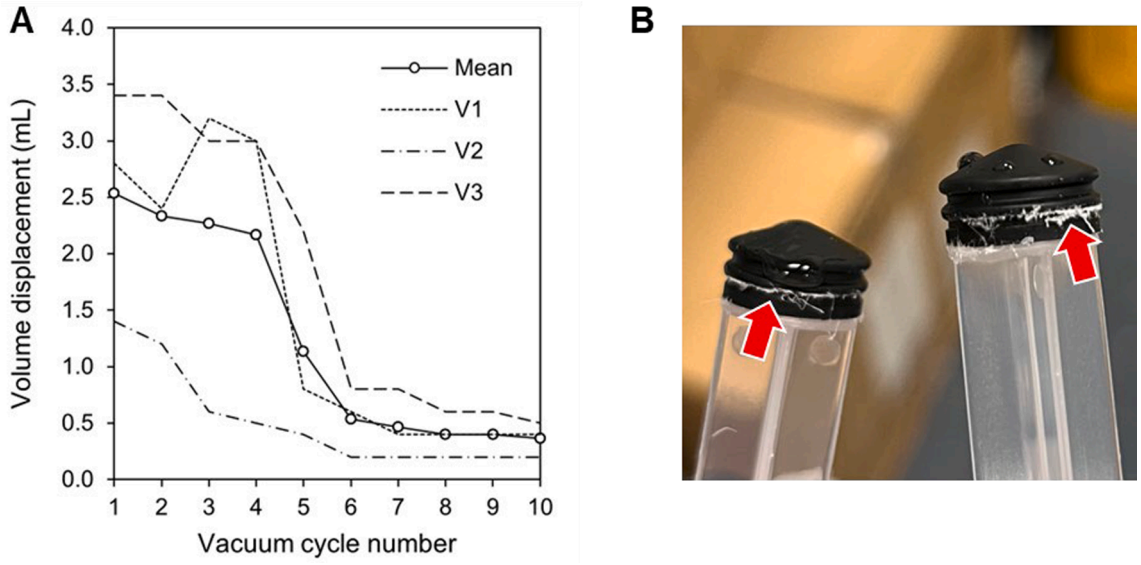

Fig. 6. (A) Lower plunger movement (as volume displacement, mL) at 100 mbar over 10 vacuum cycles with re-used syringes containing 20 % PVP solution and starting air volume = 1.1 mL. Data from 3 re-used syringes (V1, V2, V3) as well as the mean are shown. (B) White residues (indicated by arrows) on the re-used plungers following the procedure that produced the data in (A).

which the plunger cleared the 0.9 mL mark) was measured in this experiment because the plunger moved in a variable and unpredictable rate. When the experiment was initially performed with 2 mL of air in the re-used syringes, the lower plunger was ejected completely from the syringe barrel at pressures > 100 mbar in some cases, but barely moved in others at 100 mbar. Thus, the air volume within the re-used syringes was reduced to 1.1 mL to prevent this, and the plunger movement at 100 mbar (instead of the pressure at which the plunger cleared the 0.9 mL mark) was used because it was a more measurable endpoint.

On average, in the first vacuum cycle, the re-used lower plunger was displaced by 2.53 mL, which was comparable to the new syringes. This movement then decreased over the next 3 cycles and by the 5th cycle, the plunger had moved 56 % less than in the first cycle. By the 10th cycle, it had moved 86 % less compared to the first cycle.

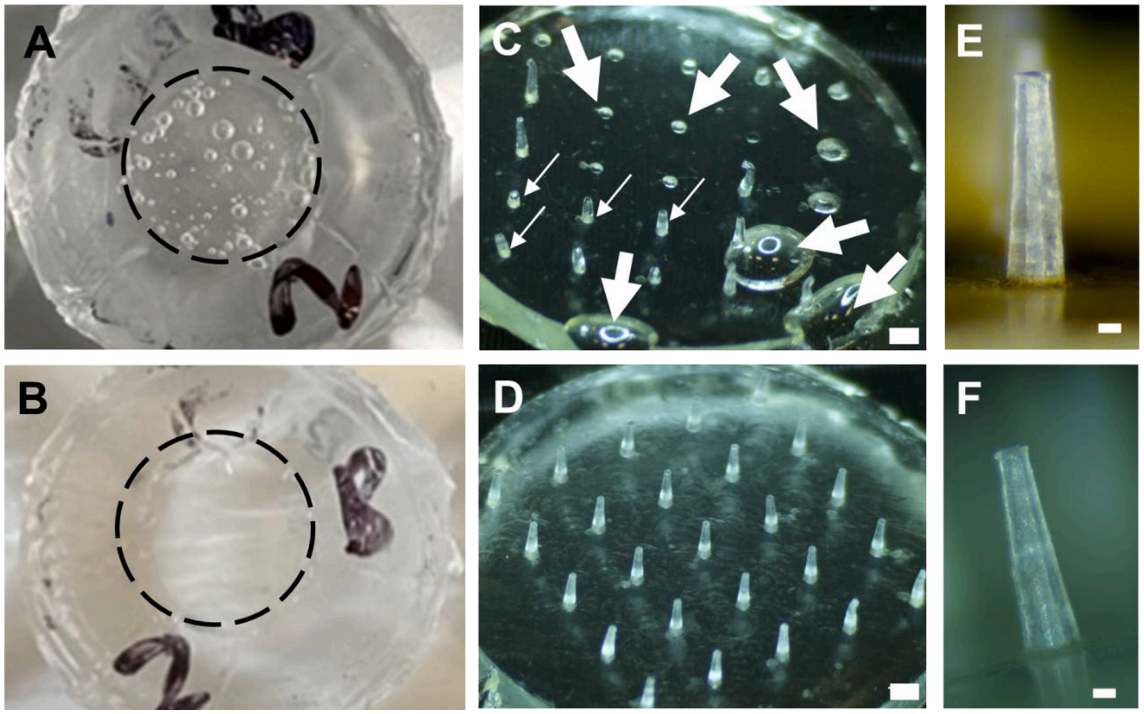

Fig. 7. (A–B) Representative images of filled microneedle moulds containing 20 % PVP solution immediately before drying: (A) after 45 min at 100 mbar using the conventional 'fill-and-vac' method, (B) after the new 'vac-and-fill' method. The liquid formulation was contained within the region demarcated by the dashed circle in both cases. Air bubbles were visible in (A) but not in (B). (C–D) Representative images showing PVP microneedle arrays fabricated using (C) the conventional 'fill-and-vac' micromoulding technique and (D) the new 'vac-and-fill' technique. The thin arrows in (C) indicate malformed microneedles that were variable in length and shorter than expected, while the thick arrows indicate entrapped air bubbles, some of which prevented microneedle formation, in contrast with the full array of well-formed microneedles in (D). (E) A close-up lateral view of a single microneedle on the resin master array and (F) a PVP microneedle formed using the 'vac-and-fill' technique against the resin master. Scale bars = 1 mm (A–D), 100 μm (E–F).

When the re-used syringes were examined visually after the experiment, white residues were observed at the rubber tips of the lower plungers (Fig. 6B). These residues were not visible before the experiment, and they were not present when new syringes were used.

3.3. Formation and characterisation of microneedle arrays

Video S1 (Supplementary Information) shows a PDMS microneedle mould being filled with 20 % PVP solution under vacuum using the 'vac-and-fill' method. Fig. 7 shows a comparison between the same PDMS mould filled with 20 % PVP solution and the resultant microneedle arrays produced using either the conventional 'fill-and-vac' method or the new 'vac-and-fill' method. Unlike the conventional method (Fig. 7A), the new method (Fig. 7B) did not produce visible air bubbles in the liquid formulation. This led to microneedle arrays with well-formed microneedles and no entrapped air bubbles in the backing material (Fig. 7D). In contrast, the conventional 'fill-and-vac' technique produced defective microneedle arrays, despite the lower pressure applied (Fig. 7C). Air bubbles were visible in the backing material of these microneedle arrays, as well as where the microneedles should have been, as the air bubbles often prevented microneedle formation altogether. Where the microneedles did form, many were shorter than expected and inconsistent in length.

The AFF of the PVP microneedles formed using the 'vac-and-fill' method was 0.9779 ± 0.1123 N (n = 40). It has been reported that microneedles require application forces ranging from 0.08 N to 3.04 N per microneedle to penetrate the skin successfully (Park et al., 2005). Although the application force required is dependent on the microneedle array design (e.g., geometry, pitch, aspect ratio), the measured AFF provided some confidence that the PVP microneedles would be able to penetrate the skin. Successful penetration of the PVP microneedles into porcine skin was subsequently confirmed by OCT imaging (Fig. 8). The tendency for the microneedle arrays to cling to the skin during removal provided further evidence of successful skin penetration.

Following the initial method development using the 20 % PVP solution, other microneedle arrays were fabricated with additional liquid formulations, with or without MB or DSP as the drug payload, to demonstrate the versatility of the 'vac-and-fill' method. These microneedle arrays also showed well-formed microneedles, with no visible air bubbles (Fig. 9). Notably, the various PMVE/MA and HEC liquid formulations used to produce these microneedle arrays were more viscous than the 20 % PVP formulations (Table 1). The result thus demonstrates that the 'vac-and-fill' method can be used to fabricate microneedle arrays from liquid formulations across a wide viscosity range.

4. Discussion

Removing air (degassing) from the mould by centrifugation or vacuum after filling provides a convenient workflow. However, the centrifugation method is limited by the size of rotors and could cause unwanted sedimentation (Yang et al., 2012). It is also more time-consuming and labour-intensive than the vacuum method (Chen et al., 2019). Therefore, the vacuum method ('fill-and-vac') is used to circumvent these limitations. In our experience, the conventional 'fill-and-vac' method has led to entrapped air bubbles and malformed microneedles, despite multiple prolonged vacuum cycles (Fig. 3, Fig. 7A and Fig. 7C). We did not find many reports of this problem in the literature, possibly due to publication bias, since negative experimental outcomes are generally less likely to be published than positive ones (Nissen et al., 2016). Whilst others have successfully formed microneedle arrays using various versions of the 'fill-and-vac' micromoulding method, the process parameters are often not fully described. For example, for degassing after mould-filling, Tas et al. (2017) applied 27 mmHg (36 mbar) for an unspecified duration, while Lau et al. (2017) applied an unspecified pressure for 3–5 min. They also generally used low polymer concentrations, which would produce solutions of relatively low viscosity (e.g., Tas et al. (2017) used a 7.5 % (w/v) PVP solution). Using a lower polymer concentration may mitigate the problem by reducing the viscosity of the liquid formulation, thus encouraging liquid flow and the removal of air bubbles through the liquid but may be detrimental to the physical properties of the microneedles, depending on the formulation. Reducing polymer concentration may produce a more porous structure upon drying (Galiano, 2014; Tan and Rodrigue, 2019), thereby reducing the mechanical strength of the microneedles. Moreover, a lower polymer concentration is usually achieved by using a larger volume of solvent, which consumes more energy and time to dry. It may also lead to significant shrinkage of the microneedles upon drying (Katsumata et al., 2013). In any case, the process parameters of micromoulding are likely to be formulation- and equipment-dependent and therefore some modifications will be necessary per formulation, especially when attempting to reproduce such processes in different laboratories with different equipment capabilities.

From the positions of the air bubbles and the resultant microneedle arrays (Fig. 3 and Fig. 7C), the entrapped air and malformed microneedles seen with the conventional 'fill-and-vac' method were clearly a result of insufficient air evacuation from the microcavities of the PDMS moulds. Once a liquid formulation has been loaded over the microcavities, the degassing step is intended to drive the entrapped air out of the microcavities, so that it rises through the body of the liquid to escape through the surface. This transit could potentially be impeded by several factors, including the viscosity and depth of the liquid formulation (and thus the transit rate and distance), the size and shape of the

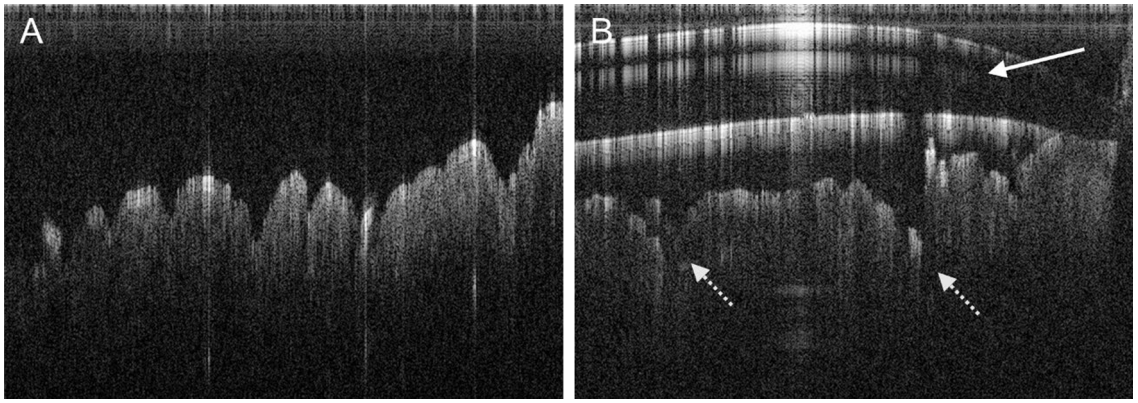

Fig. 8. OCT images of (A) pig skin before microneedle insertion, (B) PVP microneedles made using the 'vac-and-fill' method inserted into pig skin. The PVP microneedle array was left in situ during OCT imaging (solid arrow). The microneedles in the pig skin and the micropores thus created are indicated by the dashed arrows.

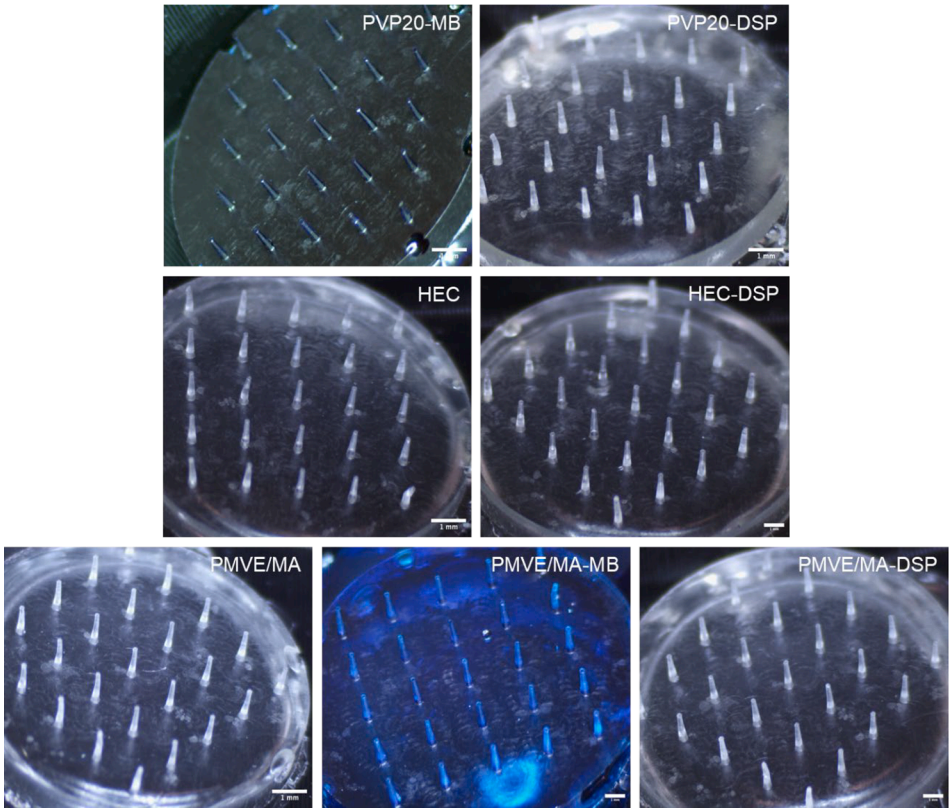

Fig. 9. Light micrographs of microneedle arrays fabricated from a range of polymers using the 'vac-and-fill' method, with or without MB or DSP as the drug payload. Scale bar = 1 mm.

microcavities (and thus the amount of air that needs to be evacuated and how easy it is for the air to leave the microcavities), the volatility of the liquid formulation (low pressures tend to accelerate evaporation, thus increasing the viscosity of the polymeric liquid formulation under vacuum), and gelation behaviour (which increases the viscosity of the liquid formulation in a time-dependent manner). To circumvent these potential problems, we decided to take an alternative approach by evacuating the air from the microcavities first before filling the mould (i.e., the 'vac-and-fill' method). The challenge with this approach was that the mould would need to be filled within the enclosed vacuum chamber, which would make manual handling extremely challenging. Martin et al. (2012) addressed this by manually injecting the liquid formulation through a rubber septum covering a vacuum flask, in which the mould was held at 100 mbar for 30 min prior to the injection. However, the introduction of the injection device through the septum entails momentarily breaching the airtight seal afforded by the rubber septum, potentially altering the pressure. Viscous liquids are also generally difficult to extrude through narrow injection devices and may clog them. Furthermore, manual handling inevitably introduces inter-operator variability. Instead, we overcame this challenge by leveraging the air expansion within the syringe, in response to the controlled pressure drop within the enclosed vacuum chamber, to trigger mould-filling at the correct pressure, thus removing the need for manual handling.

For the apparatus (Fig. 1) to perform reliably, the initial volume of air in the syringe must be calibrated carefully to trigger mould-filling at an adequately low pressure. If the mould is filled at too high a pressure, the air may not have been sufficiently evacuated from the microcavities. We first addressed this concern by demonstrating that the plunger moved consistently over 10 vacuum cycles in response to the pressure drop when the syringe was filled with air alone. However, since any liquid formulation added to the syringe would be located between the expanding air and the moving lower plunger, it could potentially affect the plunger movement. For example, a viscous, sticky, and incompressible liquid could resist flow and hinder the plunger moment by compressing the air in the syringe instead. It was therefore important to demonstrate that the plunger movement was also consistent in the presence of liquid formulations of differing viscosity. We demonstrated this with — in an increasing order of viscosity — deionised water, a 20 % PVP solution, glycerol and a 40 % PVP solution (Fig. 4). In these experiments, the pressure at which the lower plunger cleared the 0.9 mL mark was recorded and was also found to be consistent over 10 vacuum cycles (Fig. 4). The 0.9 mL mark was selected as the endpoint because the 4 mm drilled hole spanned the 0.9–1.1 mL marks on the syringe, and the 0.9 mL mark was where the hole would be fully uncovered to allow the liquid formulation to flow into the mould. With 0.5 mL liquid formulation and 2 mL air in the syringe, the lower plunger cleared the 0.9 mL mark between 300 and 450 mbar, depending on the formulation. Notably, this was enough to evacuate the air from the microcavities sufficiently to prevent air bubbles and malformed microneedles in the final product (Fig. 7B and Fig. 7D), considering that most reports of successful degassing operations employed much lower pressures.

Regarding the calibration, the rate of the lower plunger movement was dictated by the initial air volume in the syringe, assuming that the liquid formulation and the syringe parts were incompressible and non-deforming. In principle, the initial air volume may be approximated from Boyle's Law (Webster, 1965), which describes an inverse relationship between the volume (V) of an ideal gas and the pressure (P) it exerts at a constant temperature in a closed system (Equation (1).

$$P \propto 1/V \tag{1}$$

In practice, the air in the apparatus (Fig. 1) was expected to deviate somewhat from this relationship, complicated by other factors such as friction between the moving parts and the hydrodynamic properties of the liquid formulation (Feng et al., 2023). Since these factors were not fully accounted for in this study, calibration was initially performed iteratively by trial and error instead, using syringes containing air only

(without liquid formulation) and the relationship in Equation (1) as a guide. This was followed by a full calibration study to establish the relationship between the initial air volume and the anticipated fill pressure (see Supplementary Information). An initial air volume of approximately 2 mL was found to be suitable for uncovering the hole at approximately 300 mbar, and thus 2 mL of air was used in the rest of this study. Martin et al. (2012) also used 300 mbar in their unsuccessful attempt to form microneedles using the conventional 'fill-and-vac' method. In their improved vacuum deposition method, 100 mbar (i.e., 200–350 mbar lower than the fill pressure reported here) was used to successfully produce complete arrays of well-formed microneedles that were mechanically strong enough to penetrate the skin. Thus, at least from this perspective, the 'vac-and-fill' method reported here appears to be superior with its less demanding vacuum requirement, which requires less energy to sustain.

There was no apparent correlation between the viscosity of the liquid formulation and the fill pressure (Fig. 5). In other words, a more viscous liquid did not always impede the plunger movement more than a less viscous liquid did. For example, although the fill pressure for deionised water was generally greater than that for glycerol, the less viscous 20 % PVP apparently cleared the 0.9 mL mark at lower pressures compared to the more viscous 40 % PVP at the beginning of the vacuum cycles (Fig. 5; note that this apparent difference between 20 % PVP and 40 % PVP was only statistically significant at $p < 0.05$ in the third vacuum cycle). Whilst these data should be interpreted conservatively, considering that the pressure gauge was analogue and so the readings may not be accurate enough to draw such a firm conclusion, it is conceivable that viscosity is not the only formulation factor to potentially affect plunger movement. The relative strengths of the complex interfacial interactions between the apparatus, air and the liquid formulation are likely to play an important role. In any case, our results demonstrate that the technique can be used to fill polymer solutions of a wide range of viscosity. This was further confirmed with other PVP, PMVE/MA and HEC formulations, ranging from approximately 0.03 Pa•s to 0.45 Pa•s in shear viscosity (Table 1), all of which produced well-form microneedles using the 'vac-and-fill' method (Fig. 9).

For routine lab-scale micromoulding, the ability to re-use the syringes would make the 'vac-and-fill' method more cost-effective and sustainable due to the potential cost savings and reduction of plastic waste. However, the re-used syringes and plungers did not demonstrate the same consistency as the new syringes. The movement of the plunger was jittery, variable between the syringes and generally declined over multiple vacuum cycles (Fig. 6A). This decline in performance was probably caused by the white residue seen at the plunger tip (Fig. 6B). We have not identified the chemical that made up the white residue but suspect it to be a precipitate of the liquid formulation from the preceding study (when the syringes were new). If this formulation had not been washed out adequately, upon drying, it could have formed a thin film on the plunger tip that was difficult to see with the naked eye. It is possible that a similar film had also formed inside the syringe barrel, but we did not observe it on this occasion. During re-use, the movement of the plunger within the syringe barrel and the friction it generated could have caused the film to aggregate into the white residue which, when lodged between the plunger and the syringe barrel, prevented the plunger from moving smoothly. We note that the variability declined markedly after the 6th vacuum cycle (Fig. 6A), so it may be possible to re-calibrate the syringe for re-use. However, this remains the subject of on-going troubleshooting efforts. Based on the current data, we recommend the use of new syringes for reproducibility.

This study demonstrates that evacuating air from the mould first before filling it with the liquid formulation ('vac-and-fill') is a feasible approach to micromoulding polymeric microneedle arrays. Notably, hands-free mould-filling activated by the pressure drop allows the apparatus to be used with existing vacuum chambers without equipment modification, removes inter-operator variability, and lends itself to automation. The technique uses inexpensive consumables that are widely available (e.g., disposable plastic syringes) and equipment that is commonly used in existing micromoulding techniques (e.g., a vacuum chamber). It also does not require the very low pressures that are commonly used with the conventional 'fill-and-vac' approach. This should perhaps not be surprising because moving air through a liquid formulation, particularly a viscous one, will require more energy and thus a greater pressure differential than doing so without the liquid formulation. It could therefore also provide energy savings compared to conventional 'fill-and-vac' approaches. For large-scale production, the plastic syringes are unlikely to be appropriate or cost-effective, but could be replaced with injectors that are automatically reloaded and activated by the application of vacuum cycles. Future work should examine how the operating principles of hand-free, pressure-controlled mould-filling can be incorporated into a continuous production line to manufacture microneedle arrays efficiently.

5. Conclusions

We have developed and validated a new 'vac-and-fill' technique to fabricate polymeric microneedle arrays by using the application of vacuum to trigger hands-free mould-filling. This new technique can effectively prevent air entrapment in the mould and the liquid formulation, to produce well-formed polymeric microneedle arrays consistently, at a lower pressure differential than conventional 'fill-and-vac' micromoulding techniques. It is inexpensive and uses widely available consumables and equipment, so should be easily implemented. While we have developed this technique to solve a lab-scale problem, the same underlying principles of vacuum-activated, hands-free mould-filling could be applied in designing industrial-scale micromoulding processes to manufacture polymeric microneedle arrays effectively at scale.

CRediT authorship contribution statement

Emma Smith: Conceptualization, Formal analysis, Investigation, Methodology, Visualization, Writing – original draft. **Wing Man Lau:** Funding acquisition, Project administration, Resources, Supervision, Writing – review & editing. **Tarek M. Abdelghany:** Supervision, Writing – review & editing. **Djurdja Vukajlovic:** Writing – review & editing. **Katarina Novakovic:** . **Keng Wooi Ng:** Conceptualization, Methodology, Formal analysis, Visualization, Writing – original draft, Supervision, Project administration, Funding acquisition, Resources.

Declaration of competing interest

The authors declare that they have no known competing financial interests or personal relationships that could have appeared to influence the work reported in this paper.

Data availability

Data will be made available on request.

Acknowledgements

We thank Dr Yan Wang and Xiang Li (University of Brighton, UK) for the steel master microneedle array. We also thank Nour Nakeshbandi and Begho Obale (both of Newcastle University) for their assistance with the fabrication and characterisation of the microneedle arrays. We are grateful to colleagues at NU Farms (Newcastle University, UK) for providing the pig ears for this study.

Funding

This work was supported by The Engineering and Physical Sciences Research Council, United Kingdom (grant number EP/T517914/1) and The Northern Accelerator, United Kingdom (grant number NACCF-271).

Appendix A. Supplementary data

Supplementary data to this article can be found online at https://doi.org/10.1016/j.ijpharm.2023.123706.

References

Abdelghany, S., Tekko, I.A., Vora, L., Larrañeta, E., Permana, A.D., Donnelly, R.F., 2019. Nanosuspension-based dissolving microneedle arrays for intradermal delivery of curcumin. Pharmaceutics 11, 308. https://doi.org/10.3390/pharmaceutics11070308.

Al Khateb, K., Ozhmukhametova, E.K., Mussin, M.N., Seilkhanov, S.K., Rakhypbekov, T. K., Lau, W.M., Khutoryanskiy, V.V., 2016. In situ gelling systems based on Pluronic F127/Pluronic F68 formulations for ocular drug delivery. Int. J. Pharm. 502, 70–79. https://doi.org/10.1016/j.ijpharm.2016.02.027.

Arora, A., Prausnitz, M.R., Mitragotri, S., 2008. Micro-scale devices for transdermal drug delivery. Int. J. Pharm., Future Perspectives in Pharmaceutics Contributions from Younger Scientists 364, 227–236. 10.1016/j.ijpharm.2008.08.032.

Chen, H., Wu, B., Zhang, M., Yang, P., Yang, B., Qin, W., Wang, Q., Wen, X., Chen, M., Quan, G., Pan, X., Wu, C., 2019. A novel scalable fabrication process for the production of dissolving microneedle arrays. Drug Deliv. Transl. Res. 9, 240–248. https://doi.org/10.1007/s13346-018-00593-z.

Donnelly, R.F., Majithiya, R., Singh, T.R.R., Morrow, D.I.J., Garland, M.J., Demir, Y.K., Migalska, K., Ryan, E., Gillen, D., Scott, C.J., Woolfson, A.D., 2011. Design, optimization and characterisation of polymeric microneedle arrays prepared by a novel laser-based micromoulding technique. Pharm. Res. 28, 41–57. https://doi.org/10.1007/s11095-010-0169-8.

Donnelly, R.F., Singh, T.R.R., Garland, M.J., Migalska, K., Majithiya, R., McCrudden, C. M., Kole, P.L., Mahmood, T.M.T., McCarthy, H.O., Woolfson, A.D., 2012. Hydrogel-forming microneedle arrays for enhanced transdermal drug delivery. Adv. Funct. Mater. 22, 4879–4890. https://doi.org/10.1002/adfm.201200864.

Donnelly, R.F., McCrudden, M.T.C., Alkilani, A.Z., Larrañeta, E., McAlister, E., Courtenay, A.J., Kearney, M.-C., Singh, T.R.R., McCarthy, H.O., Kett, V.L., Caffarel-Salvador, E., Al-Zahrani, S., Woolfson, A.D., 2014. Hydrogel-forming microneedles prepared from "Super Swelling" polymers combined with lyophilised wafers for transdermal drug delivery. PLoS One 9, e111547.

Feng, X., Wu, K.-W., Balajee, V., Leissa, J., Ashraf, M., Xu, X., 2023. Understanding syringeability and injectability of high molecular weight PEO solution through time-dependent force-distance profiles. Int. J. Pharm. 631, 122486 https://doi.org/10.1016/j.ijpharm.2022.122486.

Galiano, F., 2014. Casting Solution, in: Drioli, E., Giorno, L. (Eds.), Encyclopedia of Membranes. Springer Berlin Heidelberg, Berlin, Heidelberg, pp. 1–1. 10.1007/978-3-642-40872-4_1870-3.

Gerstel, M.S., Place, V.A., 1976. Drug delivery device. US3964482A.

Gill, H.S., Denson, D.D., Burris, B.A., Prausnitz, M.R., 2008. Effect of microneedle design on pain in human volunteers. Clin. J. Pain 24, 585. https://doi.org/10.1097/AJP.0b013e31816778f9.

Haq, M.I., Smith, E., John, D.N., Kalavala, M., Edwards, C., Anstey, A., Morrissey, A., Birchall, J.C., 2009. Clinical administration of microneedles: skin puncture, pain and sensation. Biomed. Microdevices 11, 35–47. https://doi.org/10.1007/s10544-008-9208-1.

Katsumata, R., Ata, S., Kuboyama, K., Ougizawa, T., 2013. Evaporation rate effect on starting point of shrinkage stress development during drying process in solvent cast polymer film. J. Appl. Polym. Sci. 128, 60–65. https://doi.org/10.1002/app.38132.

Kaushik, S., Hord, A.H., Denson, D.D., McAllister, D.V., Smitra, S., Allen, M.G., Prausnitz, M.R., 2001. Lack of pain associated with microfabricated microneedles. Anesth. Analg. 92, 502–504. https://doi.org/10.1213/00000539-200102000-00041.

Larrañeta, E., McCrudden, M.T.C., Courtenay, A.J., Donnelly, R.F., 2016. Microneedles: A new frontier in nanomedicine delivery. Pharm. Res. 33, 1055–1073. https://doi.org/10.1007/s11095-016-1885-5.

Lau, S., Fei, J., Liu, H., Chen, W., Liu, R., 2017. Multilayered pyramidal dissolving microneedle patches with flexible pedestals for improving effective drug delivery. J. Control. Release Challenges Adv. Microneedle Technol. 265, 113–119. https://doi.org/10.1016/j.jconrel.2016.08.031.

Lau, W.M., Ng, K.W., Sakenyte, K., Heard, C.M., 2012. Distribution of esterase activity in porcine ear skin, and the effects of freezing and heat separation. Int. J. Pharm. 433, 10–15. https://doi.org/10.1016/j.ijpharm.2012.04.079.

Lee, J.W., Park, J.-H., Prausnitz, M.R., 2008. Dissolving microneedles for transdermal drug delivery. Biomaterials 29, 2113–2124. https://doi.org/10.1016/j.biomaterials.2007.12.048.

Liu, S., Jin, M., Quan, Y., Kamiyama, F., Katsumi, H., Sakane, T., Yamamoto, A., 2012. The development and characteristics of novel microneedle arrays fabricated from hyaluronic acid, and their application in the transdermal delivery of insulin. J. Control. Release 161, 933–941. https://doi.org/10.1016/j.jconrel.2012.05.030.

Martin, C.J., Allender, C.J., Brain, K.R., Morrissey, A., Birchall, J.C., 2012. Low temperature fabrication of biodegradable sugar glass microneedles for transdermal drug delivery applications. J. Control. Release 158, 93–101. https://doi.org/10.1016/j.jconrel.2011.10.024.

McAllister, D.V., Wang, P.M., Davis, S.P., Park, J.-H., Canatella, P.J., Allen, M.G., Prausnitz, M.R., 2003. Microfabricated needles for transdermal delivery of macromolecules and nanoparticles: Fabrication methods and transport studies. Proc. Natl. Acad. Sci. 100, 13755–13760. https://doi.org/10.1073/pnas.2331316100.

Ng, K.W., Lau, W.M., Williams, A.C., 2015. Towards pain-free diagnosis of skin diseases through multiplexed microneedles: biomarker extraction and detection using a highly sensitive blotting method. Drug Deliv. Transl. Res. 5, 387–396. https://doi.org/10.1007/s13346-015-0231-5.

Nissen, S.B., Magidson, T., Gross, K., Bergstrom, C.T., 2016. Publication bias and the canonization of false facts. eLife 5, e21451. 10.7554/eLife.21451.

Park, J.-H., Allen, M.G., Prausnitz, M.R., 2005. Biodegradable polymer microneedles: Fabrication, mechanics and transdermal drug delivery. J. Control. Release 104, 51–66. https://doi.org/10.1016/j.jconrel.2005.02.002.

Singh, P., Carrier, A., Chen, Y., Lin, S., Wang, J., Cui, S., Zhang, X., 2019. Polymeric microneedles for controlled transdermal drug delivery. J. Control. Release 315, 97–113. https://doi.org/10.1016/j.jconrel.2019.10.022.

Skaria, E., Patel, B.A., Flint, M.S., Ng, K.W., 2019. Poly(lactic acid)/carbon nanotube composite microneedle arrays for dermal biosensing. Anal. Chem. 91, 4436–4443. https://doi.org/10.1021/acs.analchem.8b04980.

Sullivan, S.P., Koutsonanos, D.G., del Pilar Martin, M., Lee, J.W., Zarnitsyn, V., Choi, S.-O., Murthy, N., Compans, R.W., Skountzou, I., Prausnitz, M.R., 2010. Dissolving polymer microneedle patches for influenza vaccination. Nat. Med. 16, 915–920. https://doi.org/10.1038/nm.2182.

Tan, X., Rodrigue, D., 2019. A review on porous polymeric membrane preparation. Part I: Production techniques with polysulfone and poly (Vinylidene Fluoride). Polymers 11, 1160. https://doi.org/10.3390/polym11071160.

Tas, C., Joyce, J.C., Nguyen, H.X., Eangoor, P., Knaack, J.S., Banga, A.K., Prausnitz, M.R., 2017. Dihydroergotamine mesylate-loaded dissolving microneedle patch made of polyvinylpyrrolidone for management of acute migraine therapy. J. Control. Release 268, 159–165. https://doi.org/10.1016/j.jconrel.2017.10.021.

Tucak, A., Sirbubalo, M., Hindija, L., Rahić, O., Hadžiabdić, J., Muhamedagić, K., Čekić, A., Vranić, E., 2020. Microneedles: Characteristics, materials, production methods and commercial development. Micromachines 11, 961. https://doi.org/10.3390/mi11110961.

Wang, R., Jiang, G., Aharodnikau, U.E., Yunusov, K., Sun, Y., Liu, T., Solomevich, S.O., 2022. Recent advances in polymer microneedles for drug transdermal delivery: Design strategies and applications. Macromol. Rapid Commun. 43, 2200037. https://doi.org/10.1002/marc.202200037.

Webster, C., 1965. The discovery of Boyle's law, and the concept of the elasticity of air in the seventeenth century. Arch. Hist. Exact Sci. 2, 441–502. https://doi.org/10.1007/BF00324880.

Xie, Y., Xu, B., Gao, Y., 2005. Controlled transdermal delivery of model drug compounds by MEMS microneedle array. Nanomed. Nanotechnol. Biol. Med. 1, 184–190. https://doi.org/10.1016/j.nano.2005.03.001.

Yang, S., Feng, Y., Zhang, L., Chen, N., Yuan, W., Jin, T., 2012. A scalable fabrication process of polymer microneedles. Int. J. Nanomed. 7, 1415–1422. https://doi.org/10.2147/IJN.S28511.

Zhao, X., Li, X., Zhang, P., Du, J., Wang, Y., 2018. Tip-loaded fast-dissolving microneedle patches for photodynamic therapy of subcutaneous tumor. J. Control. Release 286, 201–209. https://doi.org/10.1016/j.jconrel.2018.07.038.